PERGAMON

Journal of Geodynamics 33 (2002) 173–186

JOURNAL OF
GEODYNAMICS

www.elsevier.com/locate/jgeodyn

On fast multigrid iteration techniques for the solution of normal equations in satellite gravity recovery

Jürgen Kusche*

Institute for Theoretical Geodesy, University of Bonn, Nußallee 17, 53115 Bonn, Germany

Abstract

Dedicated satellite-to-satellite tracking (SST) or gradiometry missions like GRACE and GOCE will provide gravity field information with unprecedented resolution and precision. It has been recognized that better gravity field models and estimates of the geoid are useful for a wide range of research and application, including ocean circulation and climate change studies, physics of the Earth's interior and height datum connection and unification. The computation of these models will require the solution of large and non-sparse normal equation systems, especially if "brute force" approaches are applied. Evidently, there is a need for fast solvers. The multigrid approach is not only an extremely fast iterative solution technique, it yields, en passant, a well-defined sequence of coarser approximations as a byproduct to the final gravity field solution. We investigate the implementation of multigrid methods to satellite data analysis using space-domain representations of the anomalous gravity field. Multigrid algorithms are considered as stand-alone solvers as well as for the construction of preconditioners in the conjugate gradient technique. Our numerical results, concerning two regional gravity inversions from simulated GRACE and GOCE data, show that multigrid solvers run much faster than conjugate gradient solvers with conventional preconditioners.

1. Introduction

The gravity recovery and climate experiment (GRACE) and the gravity field and steady-state ocean circulation explorer (GOCE) satellite missions will provide gravity field information with unprecedented resolution and precision. It has been recognized that better gravity field models and estimates of the geoid are useful for a wide range of research and application, including ocean circulation and climate change studies, physics of the Earth's interior and height datum

* Tel.: +49-228-73-3578; fax: +49-228-73-3029.
E-mail address: kusche@uni-bonn.de (J. Kusche).

0264-3707/02/$ - see front matter
PII: S0264-3707(01)00062-X

connection and unification (NRC, 1997; ESA, 1999). The computation of these models from intersatellite-tracking and gradiometric data will require the solution of large normal equation systems[1]

$$\mathbf{N}\mathbf{x} = \mathbf{y} \tag{1}$$

where $\mathbf{x}$ is the vector of u unknown gravity field parameters, $\mathbf{N}$ is the $u \times u$ normal matrix and $\mathbf{y}$ is the right-hand side accumulated from satellite data. Especially if "brute force" approaches are applied, $\mathbf{N}$ will be non-sparse. Moreover, with the inherent ill-posedness of the downward continuation process, the normal matrices tend to be ill-conditioned. Therefore, one usually regularizes the problem. Applying Tykhonov-regularization with parameter α and matrix $\mathbf{M}$, the normals appear as

$$(\mathbf{N} + \alpha\mathbf{M})\mathbf{x} = \mathbf{y}. \tag{2}$$

In GRACE and GOCE data analysis the size of the system (1) or (2) will be of the order $u \sim 20{,}000 \ldots 90{,}000$, if one aims at global solutions. Besides, the optimal value of α will be unknown a priori and has to be determined from parameter choice rules like generalized cross—validation, the L-curve method or Morozov's dicrepancy principle (Xu and Rummel, 1994; Xu, 1998), if one is willing to go beyond the simple Kaula regularization. Then (2) has to be solved several times and for condition numbers varying over several orders of magnitude. Fast iterative solvers must be designed to handle the problem within acceptable computation time. A linear iteration of (1) or (2) reads (set $\mathbf{N} + \alpha\mathbf{M} =: \mathbf{N}^{\alpha}$)

$$\mathbf{x}^{k+1} = \mathbf{x}^{k} + \mathbf{C}(\mathbf{y} - \mathbf{N}^{\alpha}\mathbf{x}^{k}) \tag{3}$$

where $\mathbf{C}$ should approximate $(\mathbf{N}^{\alpha})^{-1}$. The iteration converges if and only if (Golub and van Loan, 1983)

$$\rho(\mathbf{I} - \mathbf{C}\mathbf{N}^{\alpha}) < 1. \tag{4}$$

The quantity ρ is the spectral radius of the iteration matrix $\mathbf{I}$–$\mathbf{C}\mathbf{N}^{\alpha}$ which coincides with the largest absolute value of the eigenvalues. A convergence rate $\rho = 0.1$, for example, means that one iteration step $\mathbf{x}^{k} \to \mathbf{x}^{k+1}$ increases the accuracy of the solution by one digit.

But the actual convergence rate of iterative techniques strongly depends on the individual structure of the normal equation system under consideration, which, on the other hand, depends on the chosen gravity field representation, the ordering scheme of the unknowns, the satellite altitude, the satellite data distribution, as well as the regularization parameter. Considering the case of space-domain gravity field representation, unfortunately the normal system (1) or (2) are neither sparse nor block-structured—which would make them suitable for block Jacobi techniques. In general, fast solvers for positive symmetric definite systems are Krylov methods like the

[1] Within this paper, vectors and matrices are denoted by bold letters ($\mathbf{x}$), elements of function spaces by uppercase letters (X), and mappings on function spaces by calligraphic letters ($\mathcal{X}$).

preconditioned conjugate gradient algorithm (PCCGA), and multigrid methods. The application of PCCGA techniques to global gravity recovery from SST and SGG is discussed by Schuh (2000), where spherical harmonics are used as basis. Moreaux (2000) uses truncated covariance functions in order to construct efficient preconditioners for (2) within the least-squares collocation approach. An iteration method for GOCE data analysis based on a problem-oriented approximative solver is presented in Klees et al. (2000). Recently, multigrid methods have been proposed for gravity recovery using a space-domain representation (Kusche and Rudolph, 2000; Kusche, in press), and shown to provide efficient preconditioners for normal equations from SST observations. In this paper, we will extend our analysis to normal equations from satellite gradiometric data.

For the construction of efficient multigrid solvers and preconditioners, it is necessary to go one step back and review the process of Galerkin discretization of the anomalous geopotential T: we assume that $T \in H$, where H is an infinite-dimensional Hilbert space equipped with a reproducing kernel $K = \sum_0^\infty \frac{2n+1}{4\pi} k_n P_n$. The reproducing kernel may be identified with a covariance function of T describing the state of knowledge of the geopotential power spectral density. A linear operator $\mathcal{A}_{(n)} : H \to \mathbb{R}^n$ is supposed to map T onto n satellite observations l_i of SST or gradiometry type, $l_i + \epsilon_i = \mathcal{A}_i T = (A_i, T)_H$. Here, $A_i \in H$ are the Riesz representers of the observation functionals, and ϵ_i denotes the noise. The regularized normal equations $(\mathcal{A}^*_{(n)}\mathcal{A}_{(n)} + \alpha\mathcal{I})T = \mathcal{A}^*_{(n)} l_{(n)}$ or

$$\mathcal{N}^\alpha T = Y \tag{5}$$

constitute a mapping of H onto itself, where $\mathcal{A}^*_{(n)}$ is the adjoint operator of $\mathcal{A}_{(n)}$ and $\mathcal{I}$ is the identity operator. For numerical purposes, they always have to be discretized in the sequel. One of the most popular techniques is Galerkin least-squares projection: looking for a solution T_j in a finite-dimensional subspace $H_j \in H$, one has to solve the H_j-equations

$$\mathcal{N}^\alpha_j T_j = Y_j \tag{6}$$

where $\mathcal{N}^\alpha_j$ is the restriction of the normal equation operator and Y_j is an orthogonal projection of the right-hand side (Kress, 1989). After introducing a basis, $H_j =$ span $\{\Phi_i, i = 1..u_j\}$, the nor-mals finally take the well-known form (2) with the design matrix $\mathbf{A}_{ij} = \mathcal{A}_i \Phi_j = (A_i, \Phi_j)_H$, normal matrix $\mathbf{N} = \mathbf{A}^T\mathbf{A}$,, right—hand side $\mathbf{y} = \mathbf{A}^T\mathbf{l}$,, and regularization matrix $\mathbf{M}_{ij} = (\Phi_i, \Phi_j)_H$. Common choices for the basis of the approximation subspaces are the spherical harmonics $\Phi_j = Y_{jk}, k = -j \ldots j$ or a predefined system of harmonic kernel functions $\Phi_j = \sum_0^\infty \frac{2n+1}{4\pi} \varphi_n P_n(\cdot, q_j)$, e.g. Stokes or Newton kernels. From the least-squares collocation point of view (Tscherning et al., 1990), the natural choice of the basis in H_j is given by the Riesz representers of the observation functionals, $\Phi_j = A_j, j = 1 \ldots n$. Here we end up with a Gramian matrix $\mathbf{N}_{ij} = (A_i, A_j)_H$ and right—hand side data $\mathbf{y} = \mathbf{l}$.

Eq. (6) is our point of departure in the derivation of multigrid iterative solvers. Multigrid algorithms have to be carefully adapted to the problem under consideration, but they often run faster than Krylov methods with common algebraic preconditioners, or provide efficient preconditioners. Moreover, as a byproduct they yield a well-defined sequence of coarser approximations to the final solutions in hierarchically nested subspaces.

This paper is organized as follows: in Section 2 we recall the basic principles of multigrid methods in an abstract setting. Section 3 is devoted to the description of matrix algorithms, concerning multigrid methods as stand-alone iterative solvers and as preconditioners in the conjugate gradient technique. In Section 4 we consider the embedding of the multigrid concept in the framework of least-squares geopotential approximation on the sphere, and the application to normal equations emerging from satellite gravity anomaly recovery. Here, we restrict ourselves to space-domain representations of the anomalous gravity field. Finally two numerical examples are given, where the normal systems are computed from simulations of the GRACE and the GOCE mission scenario. A summary of performance is given in Section 5.

2. The multigrid method

The multigrid approach has been developed originally during the 1960s for the iterative solution of discrete elliptic boundary value problems. Multigrid iterations belong to the class of fastest iterations because their convergence rate is independent of the discretization width, provided that certain regularity assumptions are fulfilled. Introductory texts are Bramble (1993) or Hackbusch (1985). In the mathematical literature, some recent papers also deal with multilevel iterations for the regularized solution of ill—posed problems arising from first-kind Fredholm integral equations (King, 1992; Rieder, 1997; Hanke and Vogel, 1999).

The principle of multigrid iteration is simple: Approximate solutions with smooth errors are obtained very efficiently by applying standard relaxation methods like Richardson iteration, Jacobi overrelaxation (JOR), successive overrelaxation (SOR), symmetric SOR (SSOR), or block versions of these methods (Golub and van Loan, 1983). Here smoothness means that the short wavelengths of the errors are reasonably damped, where the error is defined with respect to the exact discrete solution of the problem. Because of the error smoothness, corrections of these approximations can be calculated efficiently on coarser grids. By grids we mean hierarchically chosen approximation spaces $H_1 \subset \cdots \subset H_{j-1} \subset H_j$. This basic idea can be used recursively by employing coarser and coarser grids. Only on the coarsest grid a direct solution is computed. The basic V-cycle-algorithm for the H_j-solution of the discretized equation

$$\mathcal{L}_j X_j = Y_j, \tag{7}$$

with $\mathcal{L}_j: H_j \to \mathrm{H}_j$, goes as follows (the name "V-cycle" will be obvious from Fig. 1, left side): the $(k+1)$th iterate is given by

$$\begin{aligned} X_j^{k+1/3} &= X_j^k + S_j(Y_j - \mathcal{L}_j X_j^k) \\ X_j^{k+2/3} &= X_j^{k+1/3} + \mathcal{R}_{j-1}\mathcal{O}_{j-1}(Y_j - \mathcal{L}_j X_j^{k+1/3}) \\ X_j^{k+1} &= X_j^{k+2/3} + \mathcal{S}_j(Y_j - \mathcal{L}_j X_j^{k+2/3}) \\ &= X_j^k + \mathcal{R}_j(Y_j - \mathcal{L}_j X_j^k). \end{aligned} \tag{8}$$

By Q_{j-1} we denote the orthogonal projection onto H_{j-1}, and $\mathcal{S}_j$ is a suitably chosen relaxation operator with smoothing property. Given X_j^k, the first step (pre-smoothing) provides $X_j^{k+1/3}$, a

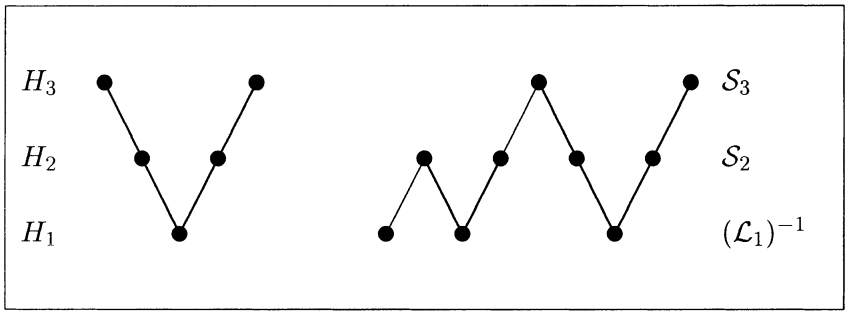

Fig. 1. Scheme of V-cycle, $j=3$ (left), and nested iteration (right).

smoothed approximation in H_j. In the second step the remaining defect, which should be of long-wavelength nature, is restricted to H_{j-1}. We apply a coarse-grid correction by $\mathcal{R}_{j-1}$. Finally a post-smoothing is performed. It should be noted that the iteration operator $\mathcal{R}_j$ is defined recursively by $\mathcal{R}_{j-1}$. Only on the coarsest space the correction needs to be solved exactly: $\mathcal{R}_1 = (\mathcal{L}_1)^{-1}$. The multigrid iteration process can be further accelerated by means of the concept of nested iteration: good initial approximations X_i^0 on each grid H_i, $i = 1..j$ can be found by performing a few multigrid steps, beginning with X_1^0. The initial coarse-space approximation "bootstraps" itself. Fig. 1 points out the principle in the case of $j=3$, which is, among the two-grid case, used in our numerical studies in Section 5.

The most crucial issue for the efficiency of multigrid algorithms is the approximation property; a Galerkin solution to in H_{i-1} should be a good long-wavelength approximation to the Galerkin solution in H_i, therefore, the coarser spaces have to be chosen in an appropriate way. Convergence proofs are usually based on Sobolev norms adapted to the problem under consideration. In order to obtain an algebraic formulation, one introduces a basis $H_j = \mathrm{span}\{\Phi_{i(j)}, i = 1..u_j\}$, and Eq. (7) leads to $\mathbf{L}\mathbf{x} = \mathbf{y}$. Within the algorithm (8), a sequence of smaller auxiliary problems $\mathbf{L}_{i-1}\delta\mathbf{x}_{i-1} = \mathbf{d}_{i-1}$ is solved instead. Due to $H_{i-1} \subset H_i$ it is clear that the base functions $\Phi_{i(j-1)}$ are spanned by the $\Phi_{i(j)}$.

$$(\Phi_{1(i-1)}, \ldots, \Phi_{u_{i-1}(i-1)})^T = R_{i-1}(\Phi_{1(i)}, \ldots, \Phi_{u_i(i)})^T, \tag{9}$$

and the auxiliary systems are related by

$$\mathbf{L}_{i-1} = \mathbf{R}_{i-1}\mathbf{L}_i\mathbf{R}_{i-1}^T \quad \mathbf{d}_{i-1} = \mathbf{R}_{i-1}\mathbf{d}_i = \mathbf{R}_{i-1}(\mathbf{y}_i - \mathbf{L}_i x_i). \tag{10}$$

The corrections are canonically "prolongated" onto the finer space H_i

$$\delta\mathbf{x}_i = \mathbf{R}_{i-1}^T\delta\mathbf{x}_{i-1} \tag{11}$$

By (11) a linear interpolation is defined. Obviously the $u_{i-1} \times u_i$ restriction matrices $\mathbf{R}_{i-1}$ determine the efficiency of the algorithm. This can be seen from the following: the projection error $\mathcal{I} - \mathcal{Q}_{i-1}$, which occurs if one simply replaces X_i by its lower-dimensional counterpart X_{i-1}, can be written using the representation (9)

$$\|\mathcal{I} - \mathcal{Q}_{i-1}\|_H = \left\|(\mathbf{M}^{-1} - \mathbf{R}_{i-1}^T(\mathbf{R}_{i-1}\mathbf{M}\mathbf{R}_{i-1}^T)^{-1}\mathbf{R}_{i-1})\mathbf{M}\right\|. \tag{12}$$

Clearly, this error should be small and confined to the high frequencies, but on the other hand $\mathbf{R}_{i-1}$ needs to be sparse with u_{i-1} as low as possible in order to preserve a low number of computer operations to set up and solve the auxiliary problems (10). Actually the restriction matrices are never stored as full matrices in order to avoid the matrix products in (10). Instead, one can use the compressed storage schemes described, e.g. in Björck (1996) very efficiently.

3. Algorithms

Based on the considerations of Section 2, a general algorithm that allows for different pre- and post-smoothing as well as multiple cycles between coarser levels, is given below:

J-grid algorithm for the solution of $(\mathbf{N} + \alpha\mathbf{M})\mathbf{x} = \mathbf{y}$ (13)

Begin : Select $\mathcal{S}, \upsilon_i, \upsilon_2, \mathbf{x}^0$
Define $\mathbf{R}_{(j)}$
do $j = J-1, .., 1$ $\mathbf{N}_{(j)} = \mathbf{R}_{(j)}\mathbf{N}_{(j+1)}\mathbf{R}_{(j)}^T$, $\mathbf{M}_{(j)} = \mathbf{R}_{(j)}\mathbf{M}_{(j+1)}\mathbf{R}_{(j)}^T$

do $k = 1, 2, ..$ $x' = \mathcal{S}^{v_1}(\mathbf{x}^{k-1}, \mathbf{y}, \mathbf{N}, \mathbf{M})$
$\mathbf{r}^{k-1} = (\mathbf{N} + \alpha\mathbf{M})\mathbf{x}' - \mathbf{y}$
$\mathbf{r}_{(J-1)} = \mathbf{R}\mathbf{r}^{k-1}$
$\delta\mathbf{x}_{(J-1)}^0 = \mathbf{0}$
do $i = 1, 2, .., \gamma$
if $J - 1 > 1$ then
$\delta\mathbf{x}_{(J-1)}^i = \mathcal{M}(\delta\mathbf{x}_{(J-1)}^{i-1}, \mathbf{r}_{(J-1)}, \mathbf{N}_{(J-1)}, \mathbf{M}_{(J-1)})$
else if $J - 1 = 1$ then
Solve $(\mathbf{N}_{(1)} + \alpha\mathbf{M}_{(1)})\delta\mathbf{x}_{(1)} = \mathbf{r}_{(1)}$
end if
end do
$\mathbf{x}'' = \mathbf{x}' - \mathbf{R}^T\delta\mathbf{x}_{(J-1)}^{\gamma}$
$x^k = \mathcal{S}^{v^2}(\mathbf{x}'', \mathbf{y}, \mathbf{N}, \mathbf{M})$
$=: \mathcal{M}(\mathbf{x}^{k-1}, \mathbf{y}, \mathbf{N}, \mathbf{M})$.

Note that the correction $\mathcal{M}(\mathbf{x}^{k-1}, \mathbf{y}, \mathbf{N}, \mathbf{M})$ is defined in recursive manner. If we choose $\gamma > 1$, algorithm (13) cycles between coarser spaces. By $\mathcal{S}^{\nu}$ we mean that a standard relaxation technique with smoothing property is applied ν times. Two standard smoothers we used in the numerical examples are

$$\mathcal{S} = \omega(\mathbf{D}^{\alpha})^{-1}\boldsymbol{y} - [(1-\omega)\boldsymbol{I} + \omega(\mathbf{D}^{\alpha})^{-1}(\mathbf{N}^{\alpha} - \mathbf{D}^{\alpha})]\mathbf{x}^{k-1}, \quad \mathbf{D}^{\alpha} = \text{diag}\,(\mathbf{N}_{ii}^{\alpha}), \tag{14}$$

$$\mathcal{S} = \alpha^{-1}\mathbf{M}^{-1}(\mathbf{y} - \mathbf{N}\mathbf{x}^{k-1}), \tag{15}$$

the first one is usually referred to as Jacobi over-relaxation. The second one essentially performs a Picard-iteration on the regularized system. Following arguments from Hackbusch (1985) and Rieder (1997), here $\upsilon_1 = 1$, $\upsilon_2 = 0$ will be chosen. The regularization matrix is usually diagonal or band-limited, so that the solution of the residual system within the Picard-smoothing can be done without problems.

On the other hand, efficient nonlinear Krylov-type solvers like the conjugate gradient method require a preconditioning strategy, if applied to equation system of bad conditions like (1) or (2). By preconditioning one means (Golub and van Loan, 1983; Hackbusch, 1993) that each CG step begins with the solution of a linear equation system,

$$\mathbf{C}_{\boldsymbol{\rho}}^{k-1} = \mathbf{r}^{k-1} \tag{16}$$

where $\mathbf{r}^{k-1} = \mathbf{N}^{\alpha}\mathbf{x}^{k-1} - \mathbf{y}$ is the residual vector and $\mathbf{C}$ is the symmetric and positive_definite preconditioner. In case of PCCGA each iteration step damps the error by $2(\sqrt{\kappa(\mathbf{C}^{-1}\mathbf{N}^{\alpha})} - 1)/(\sqrt{\kappa(\mathbf{C}^{-1}\mathbf{N}^{\alpha})} + 1)$,, (Golub and van Loan, 1983; Hackbusch, 1993), therefore, a good preconditioner should reduce the condition number κ but should also allow a fast solution of the system (16). A popular choice, which we used for comparisons in Section 5, is the diagonal preconditioner $\mathbf{C} = \mathbf{D}^{\alpha} = \mathrm{diag}(\mathbf{N}_{ii}^{\alpha})$. If one applies m cycles of a symmetric multigrid iteration to the system

$$\mathbf{N}^{\alpha}\boldsymbol{\rho} = \mathbf{r}^{k-1} \tag{17}$$

beginning with $\rho^0 = \mathbf{0}$, the preconditioner $\mathbf{C}$ is given implicitly by the m-th power of the multigrid iteration matrix, and the preconditioned residual $\boldsymbol{\rho}^{k-1}$ is the m-th multigrid iterate $\boldsymbol{\rho}^m$ for the exact solution $\boldsymbol{\rho}$ of the system (17).

We only mention that it is possible to avoid an explicit formation of the normal matrix $\mathbf{N}$ for algorithm (13), if the design matrix $\mathbf{A}$ is accessible. In this case one might begin with setting up $\mathbf{A}_{(J-1)} = \mathbf{A}\mathbf{R}_{(J-1)}^{T}$ and replace the auxiliary low-ensional normals by $\mathbf{N}_{(J-1)} = \mathbf{A}_{(J-1)}^{T}\mathbf{A}_{(j-1)}$. Computation and restriction of the defect vector within the kth iteration step then simply reads $\boldsymbol{r}_{(J-1)} = \mathbf{A}_{(J-1)}^{T}(\mathbf{A}\mathbf{x}' - 1) + \alpha\mathbf{R}_{(J-1)}\mathbf{M}\mathbf{x}'$. In Björck (1996) it is shown, how to modify the standard smoothers for this case.

4. Solution of satellite normal equations by multigrid methods

Here the basic concepts presented in the last section will be embedded in the framework of least-squares approximation on the sphere. We will apply the multigrid concept to normal equation systems emerging from satellite-related gravity data. We assume that our approximation space H_J will be spanned by a basis of isotropic harmonic functions $\Phi_{k(j)} \in H$ defined on a suitably chosen Bjerhammar sphere Ω, which allow the following Legendre series representation

$$\Phi_{k(j)} = \Phi_{(j)}(\,\cdot\,, qk) = \sum_{n=0}^{\infty} \frac{2n+1}{4\pi} \varphi_n^j P_n(\,\cdot\,, qk) \quad k = 1 \ldots u_j, \tag{18}$$

where P_n are the Legendre polynomials, φ_n^j are the Legendre coefficients, and $qk \in \Omega, k = 1 \ldots u_j$ is a set of points on the sphere. It seems natural to assume that the entries of the restriction matrix in Eq. (9) will be taken from a spherical isotropic L^2-function

$$\mathbf{R}_{ik} = R(qi, qk) = \sum_{n=0}^{\infty} \frac{2n+1}{4\pi} r_n P_n(q_i, q_k) \tag{19}$$

which should be of local support in order to minimize the computational burden. Following this line one observes that for $u_j \to \infty$ the coarse grid functions $\Phi_{k(j-1)}$ tend towards low-pass filtered versions of the $\Phi_{k(j)}$, see Kusche and Rudolph (2000).

Our numerical examples refer to regional recovery of gravity anomalies from intersatellite tracking data or satellite gradiometry data, so first we present the underlying recovery technique. Based on the generalized Stokes formula, we have a representation of the anomalous gravity field

$$T = \frac{R}{4\pi} \int_{\Omega} \delta g S(\,\cdot\,, q') \mathrm{d}\omega' \tag{20}$$

where R is the mean radius of the earth, $S(\,\cdot\,, q')$ is the extended Stokes function, and δg are generally surface gravity anomalies (Heiskanen and Moritz, 1967). In our case, they should be considered as residual referring to a chosen reference field. If one discretizes the anomaly function using u_j block—mean values, the integral (20) can be rewritten as

$$T_j = \frac{R}{4\pi} \sum_{i=1}^{u_j} \delta g_i S(\,\cdot\,, qi) \Delta\Omega_i \tag{21}$$

where $\Delta\Omega_i = \int_{\Delta\omega_i} \mathrm{d}\omega'$. With $\Phi_i = R\Delta\Omega_i/(4\pi) S(\,\cdot\,, q_i)$ we have a representation of the type (18). It has been used in a number of regional gravity recovery studies from satellite data. If the anomaly blocks are chosen as equi-angular with respect to the geographical coordinate system, the mid-points q_j constitute a geographical grid of width Δ. For GRACE and GOCE data analysis,Δ between 0.5 and 2° seems appropriate. Coarser grids for our multigrid algorithms can be obtained by doubling the grid width: $2\cdot\Delta, 4\cdot\Delta$, etc.

Assuming that n satellite measurements $l_i + \epsilon_i = \mathcal{A}_i T$ are given, the normal matrix in Eqs. (1) or (2) is $\mathbf{N} = \mathbf{A}^T\mathbf{P}\mathbf{A}$ where the design $\mathbf{A}$ matrix usually contains certain derivatives of the Stokes function, and $\mathbf{P}$ is a weight matrix which can be chosen from prior investigations on the measurement error's power spectral density. $\mathbf{x}$ is the vector of unknown mean gravity anomalies δg_i, and the right-hand side $\mathbf{y} = \mathbf{A}^T\mathbf{l}$ has to be accumulated from the data set. Numerous studies show that the normals need to be regularized-or prior-information has to be added, from the least-squares collocation point of view. But the choice of the "optimal" regularization parameter

α and matrix **M,** and measures to reduce discretization errors or the effect of omission zones will not be discussed in this paper. For more details see Xu (1992), Xu and Rummel (1994), Ilk et al. (1995), Xu (1998) and Kusche and Ilk (2000).

Within the nested iteration (Fig. 1) of the multigrid process, exact solutions $\mathbf{x}_{j-1}, \mathbf{x}_{j-2}, \ldots$ on the coarser approximation spaces are obtained. On the next-coarsest space with $2\cdot\Delta$ resolution, for example, the solution vector $\boldsymbol{x}_{j-1} = (\delta_{g1(j-1)}, \ldots, \delta q_{u_{j-1}(j-1)})^T$ of the auxiliary system

$$\mathbf{R}\mathbf{N}^{\alpha}\mathbf{R}^T\boldsymbol{x}_{j-1} = (\mathbf{R}\mathbf{N}\mathbf{R}^T + \alpha\mathbf{R}\mathbf{M}\mathbf{R}^T)\mathbf{x}_{j-1} = \mathbf{R}\mathbf{y} \tag{22}$$

provides a regularized least-squares solution for the smoothed gravity field representation

$$T_{j-1} = \frac{R}{4\pi}\sum_{i=1}^{u_{j-1}}\delta g_{i(j-1)}\left(\sum_{k=1}^{u_j} R(q_i, qk)S(\,\cdot\,, qk)\Delta\Omega_k\right). \tag{23}$$

In contrast, the restriction $\bar{\boldsymbol{x}}_{j-1} = \mathbf{R}\mathbf{x}$ of the final solution $\mathbf{x}$ computes regional means over the gravity anomaly function,

$$\bar{T}_{j-1} = \frac{R}{4\pi}\sum_{i=1}^{u_{j-1}}\left(\sum_{k=1}^{u_j} R(q_i, q_k)\delta g_k\right)S(\,\cdot\,, q_i)\Delta\Omega. \tag{24}$$

Within this study, we used a normalized 3-step restriction function,

$$R(q_i, q_k) = R(\psi_{ik}) = \begin{cases} a \text{ if } \psi_{ik} = 0 \\ b \text{ if } 0 < \psi_{ik} \leqslant \Delta \\ c \text{ if } \Delta < \psi_{ik} \leqslant \sqrt{2}\Delta \\ 0 \text{ if } \sqrt{2}\Delta < \psi_{ik} \end{cases}, \quad \sum_{k=1}^{u_j} R(\,\cdot\,, qk) = 1, \tag{25}$$

with suitable constants *a, b, c*. Good results were obtained with $b \approx a/4$ and $c \approx a/8$, but the overall performance is not too sensitive against this choice. As mentioned before, we store the few non-zero restriction coefficients in **R** less than 0.2% in our numerical examples—using the compressed matrix storage mode. This means, the double-sided matrix multiplication in (13) can be implemented efficiently.

5. Numerical examples

Two numerical examples demonstrate the application of multigrid stand-alone solution and preconditioning techniques to satellite gravity anomaly recovery. In the first one the satellite data **y** and normal matrix **N** have been created within a simulation study following the GRACE scenario: a low-low high-precision intersatellite tracking mission, based on the full EGM96 spherical harmonic geopotential model for orbit (at 400 km altitude) and data simulation. An analysis period of 31 days was chosen. Intersatellite range-rate measurements have been generated at a

sampling rate of 0.2 Hz and corrupted with gaussian white noise of variance of $(1\ \mu m/s)^2$. The methology is presented in Ilk et al. (1995). The same example has been used in Kusche and Rudolph (2000). In the second example **y** and **N** have been generated from a simulation of the GOCE mission, i.e. a gradiometry satellite at 250 km altitude. For simplification, we used only data of the earth-pointing (V_{zz}) component. The observations have been simulated at a sampling rate of 0.2 Hz and corrupted with coloured noise, which shows a 1/f-characteristic below a corner frequency. For details on this noise model see Koop et al. (2000). Since both missions will be continuously tracked by on-board GPS receivers, orbit errors were not taken into account.

The area under consideration was chosen to be $[57^\circ..132^\circ]\times[-24^\circ..43^\circ]$ in both cases, and the disturbing potential was modelled by $1^\circ\times1^\circ$ mean anomalies. This does not mean that we expect to recover the gravity field at this resolution with S/N ratio of 1, but a high resolution was chosen in order to demonstrate the performance of different algorithms in seriously ill-posed problems. The GRACE mission is expected to resolve the gravity field up to spherical harmonic degree of around 150 with better performance than GOCE below degree 90 (Balmino et al., 1998). GOCE, however, will resolve the gravity field up to a spherical harmonic degree of around 250. In both simulation examples regularization was necessary, and the regularization parameter was chosen in order to minimize the true mean square error—which is the optimal parameter in a simulation scenario, where the true solution is known.

In these examples various algorithms were applied:

- MGV2JOR multigrid algorithm, $J=2$, with the JOR smoother given in Eq. (14),
- MGV2R multigrid algorithm, $J=2$, with the Picard smoother given in Eq. (15),
- MGW3JOR multigrid algorithm, $J=3$, with JOR smoother, W-Cycle, $\gamma=3$,
- CGA-J conjugate gradient algorithm with diagonal preconditioner,
- CGA-MGV2JOR conjugate gradient algorithm with $m=2$ cycles of multigrid algorithm MGV2JOR as preconditioner,
- CGA-MGW3JOR conjugate gradient algorithm with $m=2$ cycles of multigrid algorithm MGW3JOR as preconditioner,

The coarser grids were obtained by standard coarsening, i.e. as $2^\circ\times2^\circ$ and $4^\circ\times4^\circ$ grid.

The initial $4^\circ\times4^\circ$ approximations as well as the final $2^\circ\times2^\circ$ approximations obtained by nested iteration and the final $1^\circ\times1^\circ$ approximations are shown in Figs. 2 and 3, (unit is mGal). When compared to the pseudo-true field from the EGM96 model, one observes that the main features are well-detected. As expected, one cannot hope to recover the gravity field at such high resolution from a GRACE—type mission (example 1, Fig. 2) with satisfying S/N ratio. Especially ocean ridge features remain invisible within this experiment. We found an rms error of l2 mGal in the weighted $2^\circ\times2^\circ$ block means and 5 mGal in the weighted $4^\circ\times4^\circ$ block means, when comparing to the correspondend EGM96-derived weighted blocks. These errors, however, are cumulative and include omission effects with respect to the full expansion of the pseudo-true field up to degree 360. Here the regularization parameter was 3% when compared to an average diagonal element trace(N)/u. In the second example (Fig. 3) an error of around 5 mGal in the weighted $2^\circ\times2^\circ$ block means and less than 3 mGal in the weighted $4^\circ\times4^\circ$ block means was found. Regularization was applied with 10% when compared to an average diagonal element trace(**N**)/u. This kind of a "regional" simulation, however, cannot take into account the fact that the recovery of longer

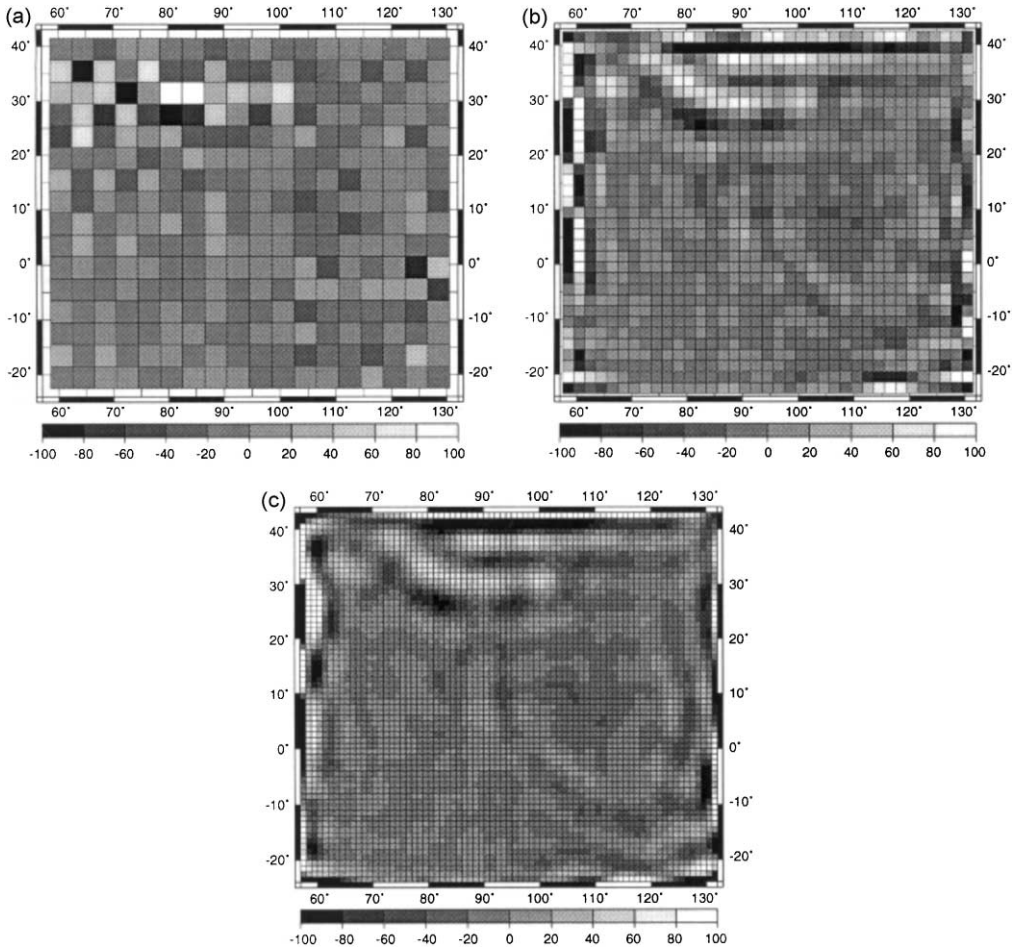

Fig. 2. (a) Initial approximation on $4^\circ \times 4^\circ$, example 1; (b) final approximation on $2^\circ \times 2^\circ$, example 1; (c) final approximation, example 1.

wavelengths of the geopotential field is generally expected to be more precisely obtained from a GRACE-type mission.

But the important result in the context of this paper is that a suitable approximation is available after only a few iteration cycles. This means that by far less than 1% computation time is required when compared to a direct solver. A comparison of the different algorithms is given in Tables 1 and 2.

Here #Iter is the number of multigrid-cycles or CG-steps required by the algorithm, and Time denotes the execution time on a SUN Ultra 1 in minutes. Each algorithm was terminated when the true rms iteration error $\left\|\mathbf{x}-\mathbf{x}^k\right\|_2$ falls below 0.1 mGal. "Exact" solutions $\mathbf{x}$, which only serve as a reference within this study, have been derived from running CGA-MGV2JOR until $\|r\|_2 < 1 \cdot 10^{-3}$.

If only two grids are implemented—which is generally favourable as long as a direct solution on the coarser space can be cheaply calculated—algorithms MGV2JOR and MGV2R run very fast

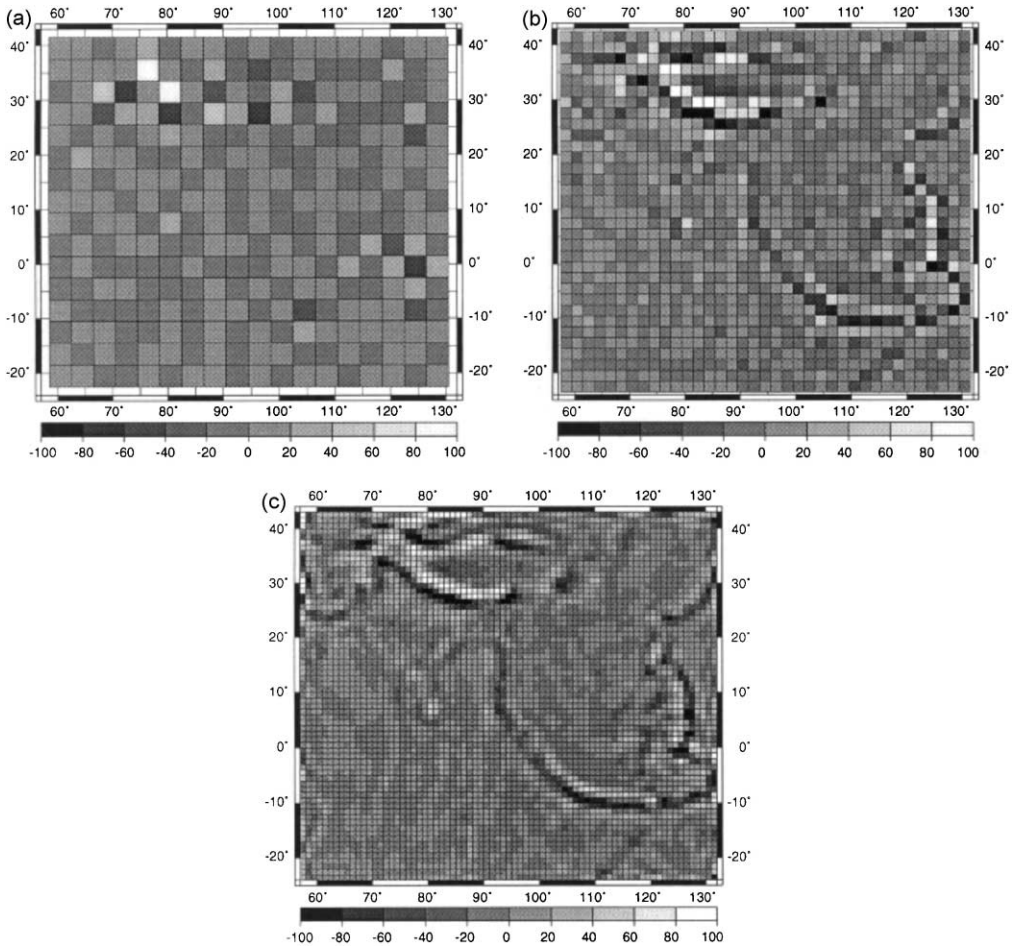

Fig. 3. (a) Initial approximation on $4^\circ \times 4^\circ$, example 2; (b) final approximation on $2^\circ \times 2^\circ$, example 2; (c) final approximation, example 2.

as long as the problem is not too severely ill-conditioned. In case of small regularization parameters or non-smooth solutions (example 2) MGV2R based on the smoother (15) diverges due to large smoothing corrections. The use of three grids serves as a test case for large-scale application. Generally we found that these algorithms (MGV3JOR and MGW3JOR) are very sensitive to the specific configuration of the smoother, i.e. v_1, v_2 and overrelaxation parameter. We believe the reason is that also the auxiliary systems in Eq. (22) are of bad condition and require careful handling. Increasing the number of inner cycles, γ, could not further enhance the performance-due to the bad condition of the auxiliary systems one would usually need $\gamma > 10$ for exact solutions which makes the algorithm perform numerically like MGV2JOR but more time-consuming. A way out, which will be investigated in a forthcoming paper, could be to choose individual regularization parameters on each grid. However, we expect that MGV3JOR and MGW3JOR have great potential for large-scale application since only systems of size less than u/16 need to be solved directly. The clear winner of this comparison is the conjugate gradient algorithm with

Table 1
Performance of different multigrid–stand-alone algorithms

	MGV2JOR		MGV2R		MGW3JOR	
	#Iter	Time	#Iter	Time	#Iter	Time
Example 1	61	41	37	25	79	80
Example 2	32	28	No convergence		44	47

Table 2
Performance of different conjugate gradient preconditioners

	CGA-J		CGA-MGV2JOR		CGA-MGW3JOR	
	#Iter	Time	#Iter	Time	#Iter	Time
Example 1	180	71	7	13	12	26
Example 2	35	2	6	12	9	21

multigrid preconditioning. We found CGA-MGV2JOR able to solve the normal equations within acceptable time even for unrealistic strong ill-posedness (for very small or even zero regularization parameters). The conjugate gradient technique with conventional preconditioning like diagonal (CGA-J) or SSOR (not shown in Table 2) could neither compete with multigrid-preconditioned CG, nor, at least not in example 1, with the linear multigrid stand-alone solvers (Table 1).

Comparing algorithmic performance in both examples we found that the overall improvement using multigrid techniques was more impressive in the first one. The reason is probably that due to the higher satellite altitude and different mission concept, one recovers a smoother gravity field solution, and consequently the coarse-level solutions are better suited to approximate the $1^\circ \times 1^\circ$ block mean solution.

References

Balmino, G., Perosanz, F., Rummel, R., Sneeuw, N., Sünkel, H., Woodworth, P., 1998. European Views on Dedicated Gravity Field Missions: GRACE and GOCE. ESA Report ESD-MAG-REP-CON-001.

Björck, A., 1996. Numerical Methods for Least Squares Problems. SIAM, Philadelphia.

Bramble, J.H., 1993. Multigrid Methods. Pitman Research Notes in Mathematics Series, Harlow.

ESA, 1999. Gravity Field and Steady-State Ocean Circulation Mission. European Space Agency Publications Division, Reports for Mission Selection, Noordwijk.

Golub, G.H., van Loan, C., 1983. Matrix Computations. John Hopkins University Press, Baltimore.

Hackbusch, W., 1985. Multi-Grid Methods and Applications. Springer Series in Computational Mathematics, Berlin.

Hackbusch, W., 1993. Iterative Solution of Large Sparse Systems of Equations. Springer Applied Mathematical Sciences, Berlin.

Hanke, M., Vogel, C.R., 1999. Two-level preconditioners for regularized inverse problems I. Theory. Num. Math. 83, 385–402.

Heiskanen, W.A., Moritz, H., 1967. Physical Geodesy. Freeman, San Francisco.

Ilk, K.H., Rummel, R., Thalhammer, M., 1995. Refined method for the regional recovery from GPS/SST and SGG. In: Study of the Gravity Field Determination using Gradiometry and GPS (Phase 2), CIGAR 111/2 Final Report, ESA contract No. 10713/93/F/FL.

King, T., 1992. Multilevel algorithms for ill-posed problems. Num. Math. 61, 311–334.

Klees, R., Koop, R., Visser, P., van den IJssel, J., Rummel, R., 2000. Data analysis for the GOCE mission. In: Schwarz: Geodesy Beyond Year 2000. JAG Symposia. Vol. 121, Springer, Berlin.

Koop, R., Visser, P., van den IJssel, J., Klees, R., 2000. Detailed scientific data processing approach. In: Sünkel, (Ed.), From Eötvös to Milligal, Final Report, ESA study, ESA/ESTEC Contract No. 13392/98/NL/GD.

Kress, R., 1989. Linear Integral Equations. Springer Applied Mathematical Sciences, Berlin.

Kusche, J., in press. Implementation of multigrid solvers for satellite gravity anomaly recovery. Journal of Geodesy.

Kusche, J., Ilk, K.H., 2000. The polar gap problem. In: Sünkel, (Ed.), From Eötvös to Milligal, Final Report, ESA study, ESA/ESTEC contract No. 13392/98/NL/GD.

Kusche, J., Rudolph, S., 2000. The multigrid method for satellite gravity field recovery. In: Schwarz (Ed.), Geodesy Beyond Year 2000, IAG Symposia Vol. 212. Springer, Berlin.

Moreaux, G., 2000. Harmonic spherical splines with locally supported kernels. In: Schwarz (Ed.), Geodesy Beyond Year 2000, IAG Symposia Vo. 212. Springer, Berlin.

NRC, 1997. Satellite Gravity and the Geosphere. National Academy Press, Washigton D.C.

Rieder, A., 1997. A wavelet multilevel method for ill-posed problems stabilized by Tikhonov regularization. Num. Math. 75, 501–522.

Schuh, W.-D., 2000. Scientific data processing algorithms. In: Sünkel, (Ed.), From Eötvös to Milligal, Final Report, ESA study, ESA/ESTEC contract No. 13392/98/NL/GD.

Tscherning, C.C., Forsberg, R., Vermeer, M., 1990. Methods for the Regional Gravity Field Modelling from SST and SGG Data. Reports of the Finnish Geodetic Institute, No. 90:2, Helsinki.

Xu, P., 1992. Determination of surface gravity anomalies using gradiometric observables. Geophys. J. tnt. 110, 321–332.

Xu, P., Rummel, R., 1994. A simulation study of smoothness methods in recovery of regional gravity fields. Geophys. J. Int. 117, 472–486.

Xu, P., 1998. Truncated SVD methods for discrete linear ill-posed problems. Geophys. J. Int. 135, 505–514.